

## Signatures of spin-glass freezing in NiO nanoparticles

S. D. Tiwari and K. P. Rajeev

*Department of Physics, Indian Institute of Technology, Kanpur 208016, India*

(Received 18 March 2005; revised manuscript received 27 July 2005; published 23 September 2005)

We present a detailed study of the magnetic properties of sol-gel prepared nickel oxide nanoparticles of different sizes. We report various measurements such as frequency, field, and temperature dependence of ac susceptibility, temperature and field dependence of dc magnetization, and time decay of thermoremanent magnetization. Our results and analysis show that the system behaves as a spin glass.

DOI: [10.1103/PhysRevB.72.104433](https://doi.org/10.1103/PhysRevB.72.104433)

PACS number(s): 75.20.-g, 75.50.Lk, 75.75.+a, 61.46.+w

### I. INTRODUCTION

For the past few decades magnetic nanoparticles have been attracting the attention of scientists from diverse disciplines from the standpoints of both fundamental understanding and useful applications.<sup>1</sup> Magnetic nanoparticles have been under scrutiny since the days of Néel<sup>2</sup> and Brown<sup>3</sup> who developed the theory of magnetization relaxation for noninteracting single domain particles. Real magnetic nanoparticles have disordered arrangement, distribution in size, and random orientation of magnetization, making their behavior very complex and challenging to understand. Effect of interparticle interaction on magnetic properties of several nanoparticle systems are available in the literature.<sup>4</sup>

In 1961 Néel suggested that small particles of an antiferromagnetic material should exhibit superparamagnetism and weak ferromagnetism.<sup>5</sup> A bulk antiferromagnet has zero net magnetic moment in zero applied field. If the surface to volume ratio, which varies as the reciprocal of the particle size, for an antiferromagnetic particle becomes sufficiently large then the particle can have a detectable net magnetic moment because of uncompensated spins at the surface. According to Néel the moment due to uncompensated spins would be parallel to the axis of antiferromagnetic alignment. If we consider a collection of such particles of varying sizes and shapes we will see that there will be a distribution of magnetic moments of different sizes, oriented randomly and interacting with each other magnetically. Thus the magnetic properties of a collection of such particles would be very different from that of the corresponding bulk material.

Following Néel it has been generally assumed that antiferromagnetic nanoparticles would show superparamagnetic behavior. For example, Ferritin, an antiferromagnetic nanoparticle, has been shown to behave as a model superparamagnet.<sup>6</sup> Its magnetization can be described by a modified Langevin function and the particle magnetic moment is found to be consistent with what is predicted by a two sublattice model usually applicable for antiferromagnetic materials.<sup>6,7</sup>

Among other antiferromagnetic nanoparticle systems NiO has been relatively well studied. It has been claimed, based on the work of Richardson and Milligan,<sup>8</sup> described in the next paragraph, that nanoparticles of NiO show superparamagnetism.<sup>9</sup> But it has also been shown that the behavior of a NiO nanoparticle system is anomalous from observations such as (i) its magnetization cannot be de-

scribed by the modified Langevin function<sup>10</sup> and (ii) its particle magnetic moment is much larger than what is predicted by the two sublattice model.<sup>11</sup> Thus the behavior of NiO nanoparticles is very different from that of ferritin. These observations motivate us to have another look at the NiO nanoparticle system.

Bulk NiO has a rhombohedral structure and is antiferromagnetic below 523 K whereas it has a cubic structure and is paramagnetic above that temperature.<sup>12</sup> Richardson and Milligan<sup>8</sup> were the first to report magnetic susceptibility measurements as a function of temperature for NiO nanoparticles of different sizes. They measured the magnetic susceptibility at a field of 3500 G and found a peak in the susceptibility much below the Néel temperature and the peak temperature was found to decrease with decreasing particle size. It was also observed that the magnetization increases with decreasing particle size. It may be noted that this work precedes the seminal work by Néel<sup>5</sup> on the superparamagnetism of antiferromagnetic particles.

In this paper we present a detailed study on NiO nanoparticles based mainly on magnetic measurements. In the course of this work we will come across phenomena which indicate that a collection of NiO nanoparticles behaves as a spin glass or as a superparamagnet. In each of those cases we shall try to critically examine the data in the light of current understanding of the physics involved.

### II. EXPERIMENTAL DETAILS

NiO nanoparticles are prepared by a sol-gel method by reacting in aqueous solution, at room temperature, nickel nitrate, and sodium hydroxide at  $pH=12$  as described elsewhere.<sup>8,10,13</sup> In this work we used nickel (II) nitrate hexahydrate (99.999%), sodium hydroxide pellets (99.99%), both from Aldrich, and triple distilled water to make nickel hydroxide. The samples of nickel oxide nanoparticles are prepared by heating the nickel hydroxide at a few selected temperatures for 3 hours in flowing helium gas (99.995%). All the magnetic measurements are done with a SQUID magnetometer (Quantum Design, MPMS XL).

### III. EXPERIMENTAL RESULTS AND DISCUSSION

#### A. Crystallite sizes

The average crystallite size is calculated by x-ray diffraction line broadening using the Scherrer formula<sup>14</sup>

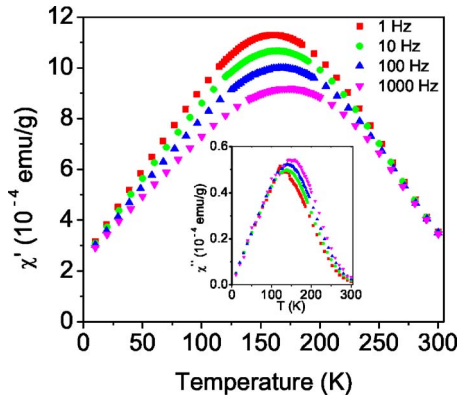


FIG. 1. (Color online) Temperature and frequency dependence of real part of ac susceptibility of 5.1 nm NiO nanoparticles. The inset shows the temperature and frequency dependence of the imaginary part of the ac susceptibility. The probing field has an amplitude of 1.0 G.

$$t = \frac{0.9\lambda}{\cos \theta_B \sqrt{B_M^2 - B_S^2}}, \quad (1)$$

where  $\lambda$  is the wavelength of the x ray (1.542 Å),  $\theta_B$  is the Bragg angle,  $B_M$  is the full width at half-maximum (FWHM) of a peak in radians and  $B_S$  is the FWHM of the same peak of a standard sample. We used specpure grade NiO powder from Johnson Matthey and Co. Ltd. (UK) as the standard. Peaks (111), (200), and (220) are used to calculate the average crystallite size. The use of  $\sqrt{B_M^2 - B_S^2}$  instead of  $B_M$  in the Scherrer formula takes care of instrumental broadening. The crystallite sizes of NiO samples prepared by heating Ni(OH)<sub>2</sub> at 250 °C, 275 °C, 300 °C, 350 °C, and 700 °C turn out to be 5.1, 5.7, 6.2, 8.5, and >100 nm, respectively, and these numbers will be referred to as the average crystallite size in this paper. Transmission electron micrograph of NiO sample prepared by heating Ni(OH)<sub>2</sub> at 250 °C gives mean particle size to be 5.6 nm with a standard deviation of 1.3 nm. We note that the mean particle size determined by transmission electron micrograph is very close to the average crystallite size determined by x-ray diffraction using the Scherrer formula (5.1 nm) which implies that on an average each NiO nanoparticle is a crystallite (tiny single crystal). More details of sample characterization like x-ray diffraction pattern, transmission electron micrograph, selected area electron diffraction pattern, and particle size distribution are available elsewhere.<sup>15</sup>

## B. ac susceptibility

### 1. Temperature and frequency dependence

The temperature dependence of ac susceptibility is measured at several frequencies ranging from 1 Hz to 1 kHz. The data are taken as described below. The sample is first cooled from room temperature to 10 K in a zero magnetic field. Then a probing ac magnetic field of 1.0 G amplitude is applied to measure the susceptibility as the temperature is slowly raised in short steps to 300 K. Figure 1 shows the real part,  $\chi'$ , of the ac susceptibility of the 5.1 nm sample; in the

inset we show the imaginary part,  $\chi''$ , which is seen to be much smaller than  $\chi'$ . We note that all the curves have a peak at some temperature; as the frequency is raised the value of  $\chi'$  decreases and the temperature of the peak increases. The behavior observed here is characteristic of both superparamagnets and spin glasses. The cusp in the ac susceptibility seen in canonical spin glasses is not observed here. This point will be discussed later in Sec. III D 2. The inset shows that below the peak temperature,  $\chi''$  does not depend on frequency. Such frequency independent  $\chi''$  has been observed in other nanoparticle systems as well.<sup>16</sup>

A quantitative measure of the peak temperature shift with frequency is the relative shift in peak temperature,  $\Delta T_p/T_p$ , per decade of frequency. For the 5.1 nm sample this quantity turns out to be 0.018. For many canonical spin glasses it lies between 0.0045 and 0.06 whereas for the known superparamagnet ferritin it has a value of  $\approx 0.13$ .<sup>17</sup> For another superparamagnet  $\alpha$ -(Ho<sub>2</sub>O<sub>3</sub>)(B<sub>2</sub>O<sub>3</sub>) a value of 0.28 has been reported for this quantity.<sup>18</sup> We note that our value of 0.018 falls in the spin-glass range.

Small particles of antiferromagnetic materials are expected to be superparamagnetic just as small particles of ferromagnetic or ferrimagnetic materials. That is, each particle would behave as a single giant moment and their magnetic susceptibility as a function of temperature would be Curie-like at sufficiently high temperature. The giant moment arises because of uncompensated spins at the surface of the particle. An antiferromagnetic particle with uniaxial anisotropy has two low energy states, separated by an energy barrier  $E_a$ , corresponding to the parallel or antiparallel alignment of the magnetization of the particle with the axis of antiferromagnetic alignment.<sup>19</sup> The susceptibility has a maximum at a certain temperature called the blocking temperature, below which the probability of thermally assisted transitions between the two low energy states decreases progressively towards zero. The blocking temperature,  $T_B$ , should increase with increasing particle size because the energy barrier separating the low energy states is proportional to the volume of the particle. In fact

$$T_B \propto V(H_K - H)^2, \quad (2)$$

where  $V$  is the volume of a single particle,  $H_K$  is a constant, and  $H$  is the field of measurement.<sup>20</sup>

The dynamics of superparamagnets is described by Arrhenius law

$$\nu = \nu_0 \exp(-E_a/k_B T), \quad (3)$$

where  $\nu$  is the rate at which the magnetization of a particle flips between the two low energy states and  $\nu_0$  is an attempt frequency that usually has a value in the range  $10^8$  to  $10^{12}$  Hz.<sup>21,22</sup> We see that the relaxation time  $\tau (=1/\nu)$  is a function of temperature and increases with decreasing temperature. If the observation time  $\tau_{\text{obs}}$  (reciprocal of the frequency,  $\nu_{\text{obs}}$ , of the probing field) is larger than  $\tau$ , the magnetization of the particle gets enough time to respond to the probing field and the response is complete. At sufficiently high temperature the above condition holds and the susceptibility increases with decreasing temperature following Curie law. At low temperature where  $\tau_{\text{obs}} \ll \tau$ , the magnetization

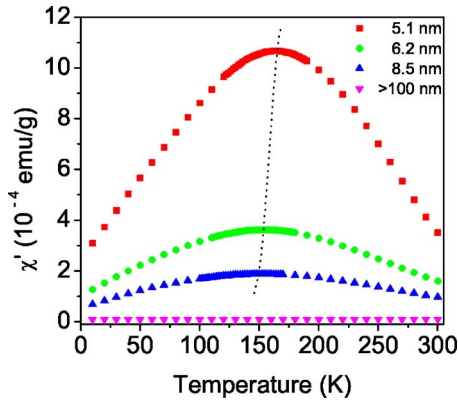


FIG. 2. (Color online) Temperature variation of the real part of ac susceptibility of NiO nanoparticles in an ac field of 1.0 G amplitude and 10 Hz frequency. The dotted line drawn to pass through the peaks shows that the peak temperature decreases with increasing particle size.

of the particle has insufficient time to respond to the applied field, the response is incomplete, the susceptibility is low, and the system is described as blocked. On increasing the temperature,  $\tau$  decreases according to the Arrhenius law, and the particle gets more time to respond to the applied field, leading to an improved response and thus the susceptibility increases with temperature at low temperature. In the region where  $\tau_{\text{obs}} \sim \tau$  (or  $\nu_{\text{obs}} \sim \nu$ ) the susceptibility goes through a peak. In real nanoparticle systems there would be a distribution of relaxation times and  $\tau$  would have to be taken as an appropriate average.

To estimate the values of  $E_a$  and  $\nu_0$  we fit the data shown in Fig. 1 to Eq. (3), where  $T$  corresponds to the peak in the susceptibility curve taken at frequency  $\nu_{\text{obs}}$ . From the fit we get  $E_a \approx 14\,500$  K and  $\nu_0 \approx 10^{39}$  Hz; these numbers are too large and rather unphysical. Unreasonable numbers like these are usually seen in spin-glass systems<sup>18</sup> while superparamagnets tend to give more reasonable numbers such as  $E_a \approx 300$  K and  $\nu_0 \approx 10^{11}$  Hz for ferritin.<sup>6</sup> Here we have another indication that the NiO particles are not behaving like a superparamagnetic system in the region of temperature where they have a susceptibility peak. This fact and the previously noted peak temperature shift with frequency suggest that the maximum in the ac susceptibility curve might have its origin in spin-glass-like freezing rather than superparamagnetic blocking.

## 2. Particle size dependence

In Fig. 2 we compare  $\chi'$  for 5.1, 6.2, 8.5, and  $>100$  nm samples at 10 Hz. It is clear that the temperature of the peak decreases with increasing particle size. This behavior is quite contrary to what is expected in superparamagnetic systems as described by Eq. (2) where  $T_B \propto$  volume of particle. We see that just as the frequency dependence of the peak temperature was unlike that of a superparamagnet, its size or volume dependence is also unlike that of a superparamagnet. In this paper we make an attempt to understand this nonintuitive behavior of NiO nanoparticles.

We also note from Fig. 2 that the magnitude of the susceptibility increases with decreasing particle size. This is as

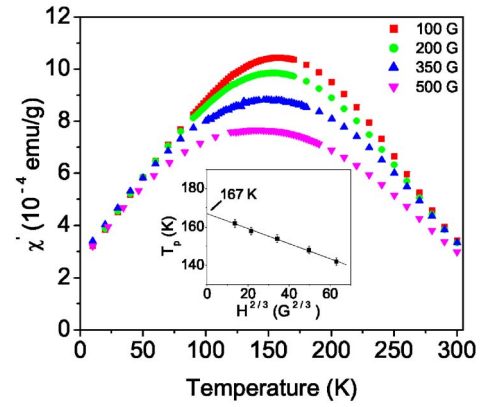


FIG. 3. (Color online) Temperature variation of the real part of ac susceptibility of 5.1 nm NiO nanoparticles at different dc fields.  $T_p$  are plotted against  $H^{2/3}$  in the inset. The solid line shows a linear fit to the data with coefficient of determination  $R^2=0.9966$ .

one would expect since the relative number of surface spins and hence the number of uncompensated surface spins would increase with decreasing particle size. Our data is in qualitative agreement with the claim that in NiO nanoparticles susceptibility at room temperature varies as  $1/d$  where  $d$  is the particle diameter.<sup>13</sup> Owing to the too few number of data points in our data set we are not able to make any quantitative claim.

## 3. Magnetic field dependence

We measured the ac susceptibility at various bias fields  $H$  with an ac field of 1.0 G amplitude and 10 Hz frequency. This is shown in Fig. 3. As  $H$  increases, the peak temperature and peak value decreases. We note that the peak temperature,  $T_p$ , decreases linearly with  $H^{2/3}$ , as shown in the inset of Fig. 3. This dependence corresponds to the so-called de Almeida-Thouless (AT) line<sup>23</sup> given by

$$H \propto (1 - T_p/T_f)^{3/2}. \quad (4)$$

The extrapolation of the AT line back to  $H=0$  gives the spin-glass transition temperature  $T_f$  which, in this case, turns out to be about 167 K. Compliance of the data with the AT line is considered to be a strong evidence for the existence of a spin-glass phase and it has been observed in different kinds of spin glasses.<sup>24</sup> Recently, it has been used as an evidence for spin-glass phase in  $\gamma\text{-Fe}_2\text{O}_3$  nanoparticles<sup>25</sup> as well as in thin films.<sup>26</sup>

## C. dc magnetization

### 1. Temperature dependence

Figure 4 shows the temperature dependence of zero field cooled (ZFC) and field cooled (FC) magnetization in a 100 G dc field for the 5.1 nm particles. Generally, the ZFC susceptibility shows a peak for both superparamagnets and spin glasses. In contrast, it is usually seen that the temperature dependence of the FC susceptibility becomes saturated below the peak temperature  $T_p$  for spin glasses and continues to increase below that temperature for superparamagnets.<sup>20</sup>

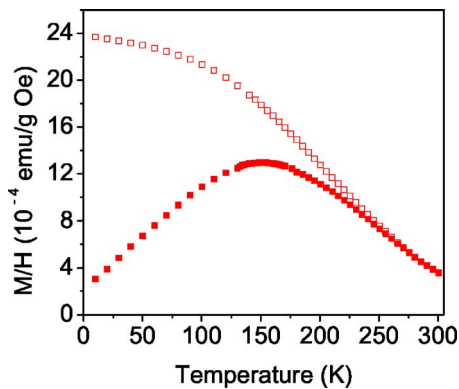


FIG. 4. (Color online) Magnetization, ZFC (solid symbol) and FC (open symbol) for 5.1 nm NiO particles as a function of temperature in 100 G field.

Nevertheless, we note that glassy behavior in magnetic nanoparticles has also been claimed in which the FC susceptibility continues to increase with decreasing temperature.<sup>27</sup> In our case, below the peak temperature, the susceptibility continues to increase but with a tendency towards saturation. This behavior is rather ambiguous.

## 2. Particle size dependence

Figure 5 shows our data on the temperature dependence of ZFC magnetization as a function of particle size in an applied field of 100 G. Clearly the peak temperature decreases with increasing particle size, as has been seen in ac susceptibility measurements in Sec. III B 2 earlier. Again, we notice the nonsuperparamagnetic behavior. A similar observation has been reported recently for MnO nanoparticles where the temperature of the peak in dc susceptibility in a zero field cooled measurement decreases with increasing particle size.<sup>28</sup>

The behavior we see here at 100 G field does not agree with the observations reported by Richardson and Milligan<sup>8</sup> on NiO where they found that at 3500 G the peak temperature in dc susceptibility increases with increasing particle size, as already mentioned in the Introduction. We did dc

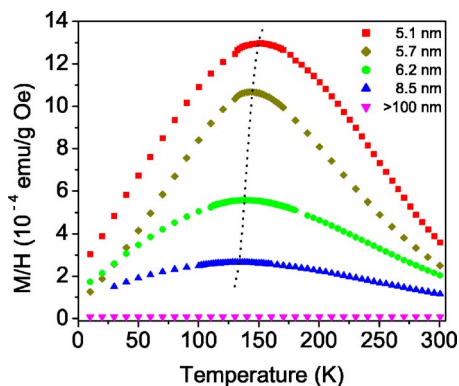


FIG. 5. (Color online) Magnetization (ZFC) as a function of temperature in 100 G applied field for NiO nanoparticles of various sizes. The dotted line, drawn to pass through the peaks, shows that the peak temperature decreases with increasing particle size.

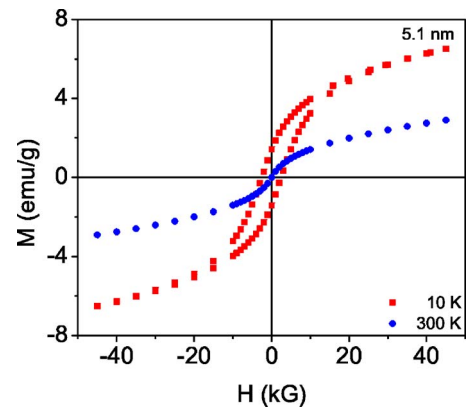


FIG. 6. (Color online)  $M$ - $H$  curves at 10 K and 300 K for the 5.1 nm particles. Hysteresis is seen in the 10 K data while there is no hysteresis at 300 K.

susceptibility measurement at 3500 G and found that we are able to reproduce<sup>15</sup> the data of Richardson and Milligan. We shall see later in Sec. III D 2 that these two conflicting observations are actually consistent with each other.

## 3. Field dependence

In Fig. 6 we show the  $M$ - $H$  curves obtained from dc magnetization measurements at 10 K and 300 K for the 5.1 nm particles. Hysteresis loop is seen in the 10 K data. The hysteresis could be an indication of the weak ferromagnetism alluded to by Néel in his musings on antiferromagnetic particles;<sup>5</sup> or it could be because the magnetization is time dependent and is relaxing too slowly for the experimental time scale of a few hours. We shall soon see that our data support the latter proposition. At 300 K there is no coercive force and no hysteresis. We carried out a few more  $M$  vs.  $H$  measurements at different temperatures up to 350 K and found that the magnetization is not a function of  $H/T$  as one would expect for superparamagnetic systems. Similar behavior has been reported by others also on NiO nanoparticles.<sup>10</sup>

In Fig. 7 we show the ZFC and FC magnetization curves for the 5.1 nm sample at various applied fields. As the measuring field increases we find that both the bifurcation temperature of ZFC and FC curves and the peak temperature of ZFC curve shift to low temperature. In fact, at 20 kG the ZFC curve does not peak even on going down to 10 K. This behavior is along expected lines since we would expect in a sufficiently high external magnetic field the spin-glass freezing will either take place at a lower temperature or not at all as such a field can break the spin-glass phase.

## 4. Time dependence

Thermoremanent magnetization (TRM) is defined as the time dependent remanent magnetization obtained when a sample is cooled from a temperature well above  $T_f$  to a temperature below  $T_f$  in an applied field  $H$  and subsequently the field is removed. In this work, to measure the TRM, we cool the sample from 300 K to the temperature of interest in a 100 G magnetic field.

A spin-glass system is not in thermal equilibrium and slowly relaxes to lower energy states. Many models have

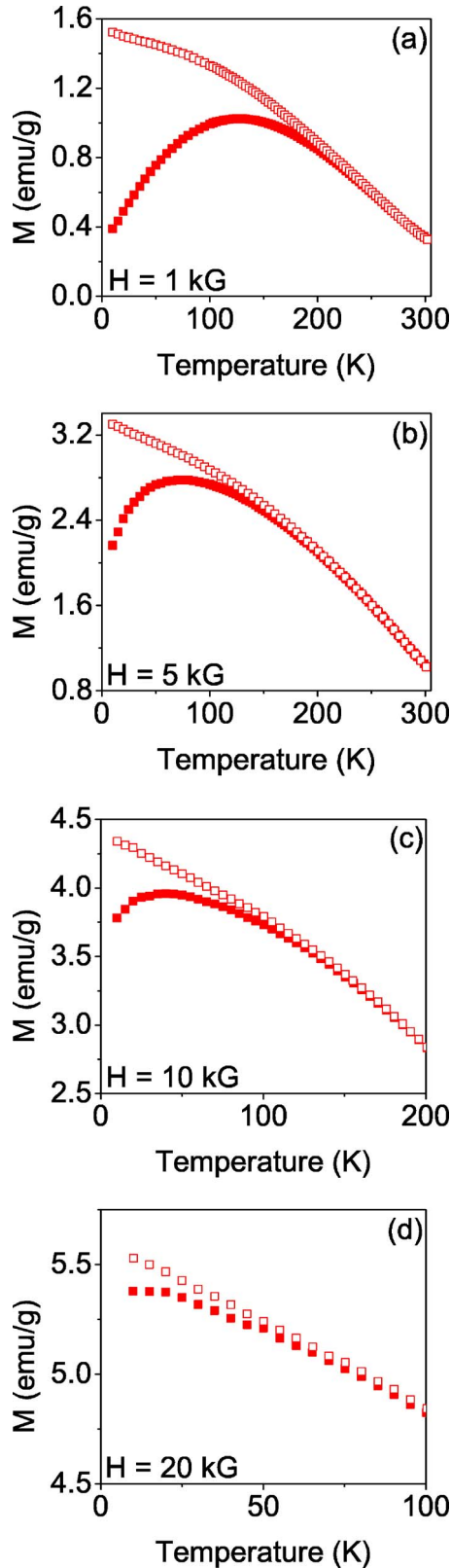


FIG. 7. (Color online) ZFC (solid symbol) and FC (open symbol) magnetization as a function of temperature in different high fields. Please note that the scales are different for each graph.

been proposed to describe the time dependent relaxation of magnetization in spin glasses. A single energy barrier should

TABLE I. Values of  $\chi^2$  and the coefficient of determination  $R^2$  obtained by fitting 100 K TRM data to various expressions for 5.1 nm sample. Total number of data points,  $N$ , is 749.

Fit expression	$\chi^2$	$R^2$
$M_0 \exp(-(t/\tau)^n)$	810	0.9998
$M_0 - S \log(t)$	1008	0.9997
$M_0 t^{-n}$	2547	0.9992

give an exponentially relaxing TRM, with time constant  $\tau$ , i.e.,  $M(t) = M_0 \exp[-(t/\tau)]$ . In a real system there would be a range of energy barriers and hence there would be a distribution of relaxation times. One of the popular forms incorporating a distribution of relaxation times is the stretched exponential function,<sup>29,30</sup>

$$M(t) = M_0 \exp[-(t/\tau)^n], \quad (5)$$

where  $\tau$  is a characteristic relaxation time and  $M_0$  and  $n$  are fit parameters.

By assuming that the energy barriers are uniformly distributed from zero to some maximum energy, it has been shown that the magnetization decays logarithmically<sup>31</sup> as

$$M(t) = M_0 - S \log(t), \quad (6)$$

where  $M_0$  and  $S$  are fit parameters. It should be noted that  $M_0$  is the magnetization at  $t=1$  unit and hence it depends on the unit of time used, while  $S$  itself does not have any such dependence.

A power law form has also been used to describe the decay of magnetization<sup>32,33</sup>

$$M(t) = M_0 t^{-n}, \quad (7)$$

where the exponent  $n$  should increase with increasing temperature. In this case also, as in the previous equation,  $M_0$  depends on the unit of time.

A statistical measure of the goodness of a fit is  $\chi^2$ , defined as<sup>34</sup>

$$\chi^2 = \sum_{i=1}^N \frac{[M_i(\text{measured}) - M_i(\text{fit})]^2}{\sigma_i^2}, \quad (8)$$

where  $N$  is the total number of data points and  $\sigma_i$  is the standard deviation of the  $i$ th data point. For a good fit  $\chi^2$  should have a value close to  $N$ . We shall also be reporting the coefficient of determination  $R^2$  for our fits; the closer  $R^2$  is to unity the better the fit.

We fitted our data to Eqs. (5)–(7). To compare the fits for the different forms we present the values of  $\chi^2$  and  $R^2$  for a representative data set, the 100 K TRM data for 5.1 nm particles, in Table I. We note that the stretched exponential gives the best fit with the lowest  $\chi^2$  and largest  $R^2$ . This is followed by the logarithmic form with the power law form bringing up the rear. To check whether the fit parameters truly characterize the data we decided to run the fits on subsets of the original data covering different time spans such as (150 s, 1000 s), (150 s, 2000 s), (150 s, 3000 s), and so on. The fit parameters are found to be strongly dependent on the time

TABLE II. Values of fit parameters  $M_0$  and  $S$  to Eq. (6) and the values of  $\chi^2$  and  $R^2$  for 5.1 nm sample at different temperatures. Total number of data points,  $N$ , is 749.

$T$ (K)	$M_0$ ( $10^{-2}$ emu/g)	$S$ ( $10^{-3}$ emu/g)	$\chi^2$	$R^2$
25	20.7	2.94	1219	0.9898
50	17.7	4.46	993	0.9979
75	14.7	6.20	1500	0.9991
100	11.9	7.06	1008	0.9997
125	8.34	6.29	2996	0.9995
150	5.54	5.02	1259	0.9998
175	3.32	3.56	10170	0.9993
200	1.73	2.32	32400	0.9991

span of the data for the stretched exponential case but are found to be almost independent of the same for logarithmic and power law cases. Consequently the stretched exponential fit must be rejected on the grounds that the fit parameters in that case are simply artifacts of the subset of the data used, even though it has the best  $\chi^2$  and  $R^2$  values.

Now we are left with the logarithmic and power law forms of which the logarithmic form has the better  $\chi^2$  and  $R^2$ . We found that Eq. (6) gives the best fit not only at 100 K, but at all the other temperatures as well. We conclude that the best fit to our TRM data is given by this equation. This equation has been popularly used to describe the time dependence of TRM of various spin-glass systems including bulk materials,<sup>31,35</sup> nanoparticles,<sup>27</sup> and thin films.<sup>26</sup> In Table II we present the results of fitting the TRM data to the logarithmic form. We see that the  $\chi^2$  is of the order of  $N$  and the  $R^2 > 0.999$  in most of the cases which reflect the high quality of the fits. It can be seen from the table that as the temperature increases the parameter  $M_0$  decreases monotonically as is to be expected. In Fig. 8 we show the thermoremanent magnetization of the 5.1 nm particles at 100 K along with the logarithmic fit. The solid line through the data points is the fit and we note that it is excellent. In the inset we plot the fit parameter  $S$ , which characterizes the relaxation rate, as a function of temperature for the 5.1 nm and 6.2 nm particles. We see that  $S$  peaks around 100 K for both samples. Peaks in  $S$  vs  $T$  curves have been seen in other spin-glass systems also.<sup>27,31</sup>

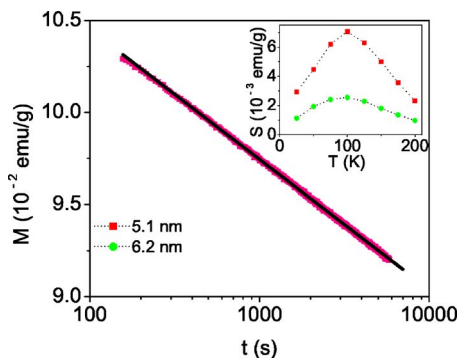


FIG. 8. (Color online) Time decay of the thermoremanent magnetization of 5.1 nm particles at 100 K. The solid line represents the fit to Eq. (6). The inset shows  $S$  as a function of temperature.

Effect of wait time dependence on TRM for spin glasses has been studied by several groups.<sup>29,36,37</sup> It is generally observed that the rate of magnetization decay decreases with increasing wait time. We also studied the wait time dependence of decay of TRM at 100 K for the 5.1 nm system. For this the sample is cooled from 300 K to 100 K in a field of 100 G and then we wait for a time  $t_w$  before the field is switched off and the data acquisition is started. In Table III we show the fit parameters to Eq. (6). It is clear that there is a small decrease in the fit parameter  $S$  for increasing wait time up to 1 hour which is consistent with others' observations.<sup>36-38</sup>

#### D. Further discussion

In Secs. III B 2 and III C 2 we saw that the peak temperature of the low field susceptibility as a function of temperature decreases with increasing particle size. We take this to mean that the behavior of the system is not superparamagnetic and the peaks in the low field susceptibility vs temperature curves are not because of superparamagnetic blocking of particle magnetic moments. From Secs. III B 1, III B 3, and III C 4 it is clear that the system is behaving as a spin glass. At this point we would like to strengthen the case that our system is showing spin-glass behavior by discussing critical scaling.

##### 1. Scaling

The dc magnetization in a spin-glass system, above the spin-glass transition temperature  $T_f$ , can be written in odd powers of the applied field  $H$  as<sup>39</sup>

TABLE III. Fit parameters  $M_0$  and  $S$  for 5.1 nm sample for different wait times  $t_w$  at 100 K.

$t_w$ (minutes)	$M_0$ ( $10^{-2}$ emu/g)	$S$ ( $10^{-3}$ emu/g)	$R^2$
0	11.9	7.06	0.9997
15	11.8	6.99	0.9994
30	11.7	6.92	0.9994
60	11.7	6.91	0.9991

$$M = \chi_0 H + \chi_2 H^3 + \chi_4 H^5 + \dots, \quad (9)$$

where  $\chi_0, \chi_2, \chi_4, \dots$  are functions of temperature. Now the dc susceptibility can be expressed in even powers of the applied field  $H$  as

$$\frac{M}{H} = \chi_0 + \chi_2 H^2 + \chi_4 H^4 + \dots. \quad (10)$$

When a spin-glass transition occurs at a temperature  $T_f$ , the linear susceptibility  $\chi_0$  is nondivergent whereas  $\chi_2, \chi_4, \dots$  diverge in the critical region (just above  $T_f$ ).<sup>39</sup> Thus to examine the possibility of critical behavior in a spin-glass system an appropriate quantity to study would be the nonlinear susceptibility,  $\chi_{NL}$ , defined as

$$\chi_{NL} = \chi_0 - \frac{M}{H} = -(\chi_2 H^2 + \chi_4 H^4 + \dots). \quad (11)$$

$\chi_{NL}$  should diverge in the critical region as  $\chi_2, \chi_4, \dots$  are divergent in that region. In a sufficiently low field (whose strength would be system dependent) the  $\chi_2$  term would dominate and in this region  $\chi_{NL}$  would vary as  $H^2$ . Near  $T_f$ ,  $\chi_2$  is expected to diverge according to the critical scaling law<sup>40</sup>

$$\chi_2 \propto t^{-\gamma}, \quad (12)$$

where  $t$  is the reduced temperature  $[(T - T_f)/T_f]$  and  $\gamma$  is a critical exponent. To describe  $\chi_{NL}$  in the critical region, the following scaling equations have been proposed:<sup>40</sup>

$$\chi_{NL} \approx t^\beta F(H^2/t^{\beta+\gamma}) \quad (13a)$$

or

$$\chi_{NL} \approx H^{2\beta/(\beta+\gamma)} G(H^2/t^{\beta+\gamma}), \quad (13b)$$

where  $\beta$  is the critical exponent of the spin-glass order parameter and  $F(x)$  and  $G(x)$  are scaling functions. To demonstrate scaling  $\beta, \gamma$ , and  $T_f$  are selected such that all the data points are judged to fall on a single curve in the best possible manner on a plot of  $\chi_{NL}/t^\beta$  or  $\chi_{NL}/H^{2\beta/(\beta+\gamma)}$  vs  $H^2/t^{\beta+\gamma}$ . As  $t \rightarrow 0$  (i.e.,  $T \rightarrow T_f$ ), the abscissa and ordinate span many decades; this prompted the early workers to make their scaling plot on a log-log scale. A logarithmic scaling plot gives equal importance to all values of  $\chi_{NL}$  although the smaller values are usually less accurate and thus the results may be misleading. It has been argued that a static scaling equation, in which the scaling function is linear in  $t$ , would test the scaling behavior in a much better fashion<sup>41</sup>

$$\chi_{NL} \propto H^{2\beta/(\beta+\gamma)} \bar{G}(t/H^{2/(\beta+\gamma)}), \quad (14)$$

where  $\bar{G}$  is the new scaling function.

Figure 9 shows the scaling plot of our data using Eq. (14). It is clear that four different data sets taken at different magnetic fields are falling reasonably well on a master curve to within experimental error. It is difficult to determine the values of  $\beta, \gamma$ , and  $T_f$  accurately that make the data points fall on a single curve.<sup>41</sup> There are several possible sets of  $\beta, \gamma$ , and  $T_f$  that would give comparably good plots. For the data shown in Fig. 9 the parameters are  $T_f = 150$  K,  $\gamma = 25$ , and  $\beta = 3.2$ . Mean field theory says that values of  $\beta$  and  $\gamma$  should

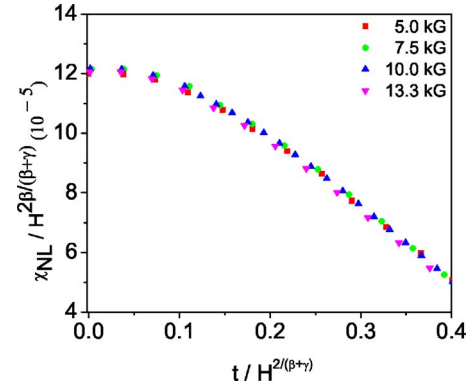


FIG. 9. (Color online) Linear scaling plot of the dc nonlinear susceptibility data for 5.1 nm NiO nanoparticles. The figure shows the curve obtained using  $T_f = 150$  K,  $\gamma = 25$ , and  $\beta = 3.2$ .  $H$  is in units of G and  $\chi_{NL}$  is in units of emu/g Oe.

be unity, however the values determined from experiments often do not agree with this and can be much larger than unity.<sup>42</sup>

At this juncture we would like to point out that our  $\chi_{NL}$  does not diverge as  $t \rightarrow 0$ . This issue will be discussed in Sec. III D 2. Now we would like to address the question of the possible mechanisms responsible for the spin-glass freezing.

## 2. Possible freezing mechanisms

There are reports in the literature where dipolar interaction between particles has been proposed as the reason for the freezing of particle magnetic moments.<sup>22,27,43</sup> Now let us examine whether there is such a possibility in the case of NiO. We estimate that for the 5.1 nm particles there would be an average uncompensated moment of the order of  $100\mu_B$ .<sup>44</sup> The maximum dipolar interaction energy between two such particles touching each other would be  $\sim 10^{-17}$  erg which corresponds to about 0.1 K on temperature scale. This means that if dipolar interaction were causing the freezing it would occur at about 0.1 K which is much lower than the observed freezing temperature of about 167 K (from ac susceptibility). Thus we rule out the possibility that dipolar interaction among particles is causing the peaks in low field susceptibility as a function of temperature.

In canonical spin glasses the spin-glass phase is very sensitive to external fields and the application of a field of a few hundred gauss makes it disappear. But here it is not the case as can be seen from Fig. 9; in fact the spin-glass phase survives up to the highest field used to measure ZFC and FC magnetization (up to 20 kG in our study; see Fig. 7). The existence of spin-glass phase up to such high fields is also evident from the AT lines shown in Fig. 10. Clearly the peak temperature of the susceptibility curve decreases with increasing applied field following the AT line. We also find that the rate of change with field of the peak temperature of the susceptibility curve decreases with increasing particle size, as shown in Fig. 11. That is, for smaller particles the  $T_p$  changes more with field than for the larger particles. It is this which gives rise to and resolves the conflicting observations noted at the end of Sec. III C 2. That is, from the fact that the AT lines cross each other, it can be easily seen that at low

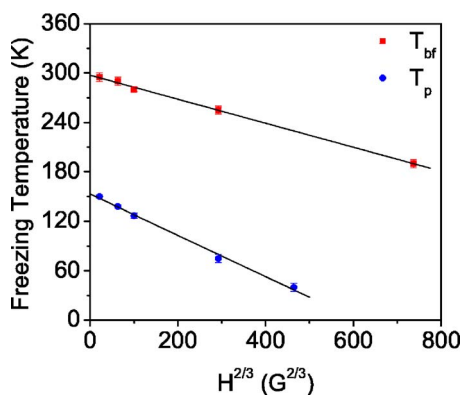


FIG. 10. (Color online) The point of bifurcation ( $T_{bf}$ ) of ZFC and FC magnetization curves is considered to be the starting point of the freezing process. The peak temperature ( $T_p$ ) in the ZFC magnetization curve is generally considered as the freezing temperature. This figure shows plots of  $T_{bf}$  and  $T_p$  vs  $H^{2/3}$ . The solid lines show linear fits to the data with  $R^2$  of 0.9984 and 0.9954, respectively. The upper and lower curves have zero field intercepts of 297 K and 153 K, respectively.

fields the peak temperature decreases with increasing particle size while the reverse happens at high fields.

Kodama *et al.*<sup>45</sup> and Martínez *et al.*<sup>25</sup> have argued that freezing of surface spins can lead to a spin-glass phase which survives up to such high fields. Kodama *et al.* have proposed a model for ferrimagnetic nickel ferrite nanoparticles where the spins at the surface of a particle are disordered, leading to frustration and spin-glass-like freezing. A similar model has also been proposed for antiferromagnetic ferrihydrite nanoparticles.<sup>46</sup> We feel that such a model may be applicable in the case of NiO nanoparticles as well. We will first have to see whether we can propose any mechanism for surface spin disorder in our case. The exchange interaction between two neighboring  $\text{Ni}^{2+}$  ions is mediated by an oxygen ion (superexchange), and if an oxygen ion is missing from the surface, the exchange bond would be broken and the interaction energy would be reduced. Also, the average coordination number for  $\text{Ni}^{2+}$  ions at the surface will be less than that in the bulk and this can result in a distribution of exchange energies for the surface spins. Moreover, the superexchange is sensitive to bond angles and bond lengths, which are likely to be different at the surface compared to that in the bulk. The reasons mentioned above may be sufficient to give rise to surface spin disorder and frustration leading to a spin-glass phase.

This mechanism of surface spin freezing can account for the absence of cusp in the ac susceptibility data (Fig. 1). We

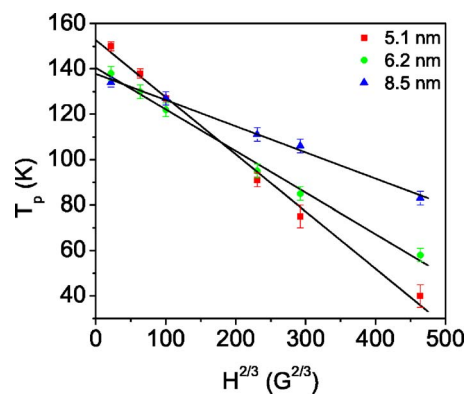


FIG. 11. (Color online) AT line for NiO nanoparticles of various sizes. The solid lines show linear fits to the data. Clearly, slope of AT lines decreases with increasing particle size or with decreasing surface disorder.

argue that there are two reasons for this. (i) A phase transition will be sharp only for an infinite system<sup>47</sup> and hence a cusp, which is an indication of a phase transition, will show up only in an infinite system. In our case, a system of a few hundred surface spins on a particle is very much finite and hence the cusp will be rounded out. (ii) The extent of surface spin disorder will be different for different particles because the particles are of different sizes and shapes. This gives rise to a distribution of freezing temperatures, further broadening the susceptibility maximum. These two reasons mentioned here will also account for the nondivergence of  $\chi_{NL}$  in the critical region (Fig. 9).

The fraction of atoms lying on the surface of the particles increases with decreasing particle size. This may lead to increased surface spin disorder as the particle size decreases and could possibly account for the increasing freezing temperature with decreasing particle size.

#### IV. CONCLUSION

In this paper we reported a detailed study on magnetic properties of sol-gel prepared NiO nanoparticles. The behavior of the system is not superparamagnetic as was expected. In fact it shows spin-glass behavior which we attribute to surface spin disorder.

#### ACKNOWLEDGMENTS

The authors thank A. K. Majumdar, Avinash Singh, and R. C. Budhani for helpful discussions.

<sup>1</sup>R. W. Chantrell and K. O'Grady, in *Applied Magnetism*, edited by R. Gerber *et al.* (Kluwer Academic, The Netherlands, 1994), p. 113.

<sup>2</sup>L. Néel, *Ann. Geophys. (C.N.R.S.)* **5**, 99 (1949).

<sup>3</sup>W. F. Brown, Jr., *Phys. Rev.* **130**, 1677 (1963).

<sup>4</sup>J. O. Andersson, C. Djurberg, T. Jonsson, P. Svedlindh, and P.

Nordblad, *Phys. Rev. B* **56**, 13983 (1997); J. L. Dormann, D. Fiorani, R. Cherkaoui, E. Tronc, F. Lucari, F. D'Orazio, L. Spinu, M. Noguès, H. Kachkachi, and J. P. Jolivet, *J. Magn. Mater.* **203**, 23 (1999); J. L. Dormann, D. Fiorani, R. Cherkaoui, L. Spinu, F. Lucari, F. D'Orazio, M. Noguès, E. Tronc, J. P. Jolivet, and A. Garcia, *Nanostruct. Mater.* **12**, 757

- (1999); C. Djurberg, P. Svedlindh, P. Nordblad, M. F. Hansen, F. Bødker, and S. Mørup, *Phys. Rev. Lett.* **79**, 5154 (1997).
- <sup>5</sup>L. Néel, in *Low Temperature Physics*, edited by C. Dewitt *et al.* (Gordan and Beach, New York, 1962), p. 413.
- <sup>6</sup>S. H. Kilcoyne and R. Cywinski, *J. Magn. Magn. Mater.* **140–144**, 1466 (1995).
- <sup>7</sup>S. A. Makhlof, F. T. Parker, and A. E. Berkowitz, *Phys. Rev. B* **55**, R14717 (1997).
- <sup>8</sup>J. T. Richardson and W. O. Milligan, *Phys. Rev.* **102**, 1289 (1956).
- <sup>9</sup>See, for example, Richardson *et al.* (Ref. 13) and references therein.
- <sup>10</sup>S. A. Makhlof, F. T. Parker, F. E. Spada, and A. E. Berkowitz, *J. Appl. Phys.* **81**, 5561 (1997).
- <sup>11</sup>R. H. Kodama, S. A. Makhlof, and A. E. Berkowitz, *Phys. Rev. Lett.* **79**, 1393 (1997).
- <sup>12</sup>J. S. Smart and S. Greenwald, *Phys. Rev.* **82**, 113 (1951).
- <sup>13</sup>J. T. Richardson, D. I. Yiagas, B. Turk, K. Foster, and M. V. Twigg, *J. Appl. Phys.* **70**, 6977 (1991).
- <sup>14</sup>B. D. Cullity, *Elements of X-Ray Diffraction* (Addison-Wesley, New York, 1956), pp. 99 and 262.
- <sup>15</sup>S. D. Tiwari and K. P. Rajeev, cond-mat/0408427, Thin Solid Films (to be published).
- <sup>16</sup>T. Jonsson, P. Nordblad, and P. Svedlindh, *Phys. Rev. B* **57**, 497 (1998).
- <sup>17</sup>Estimated by us from the data in Kilcoyne and Cywinski (Ref.6).
- <sup>18</sup>J. A. Mydosh, *Spin Glass* (Taylor and Francis, New York, 1993), pp. 65–67.
- <sup>19</sup>I. S. Jacobs and C. P. Bean, in *Magnetism*, edited by G. T. Rado and H. Suhl (Academic, New York, 1963), Vol. III, p. 271.
- <sup>20</sup>T. Bitoh, K. Ohba, M. Takamatsu, T. Shirane, and S. Chikazawa, *J. Phys. Soc. Jpn.* **64**, 1305 (1995).
- <sup>21</sup>A. Labarta, O. Iglesias, Ll. Balcells, and F. Badia, *Phys. Rev. B* **48**, 10240 (1993).
- <sup>22</sup>S. Mørup, F. Bødker, P. V. Hendriksen, and S. Linderth, *Phys. Rev. B* **52**, 287 (1995).
- <sup>23</sup>J. R. L. de Almeida and D. J. Thouless, *J. Phys. A* **11**, 983 (1978).
- <sup>24</sup>See for instance, R. V. Chamberlin, M. Hardiman, L. A. Turkevich, and R. Orbach, *Phys. Rev. B* **25**, 6720 (1982); P. Monod and H. Bouchiat, *J. Phys. (Paris), Lett.* **43**, 145 (1982).
- <sup>25</sup>B. Martínez, X. Obradors, Ll. Balcells, A. Rouanet, and C. Monty, *Phys. Rev. Lett.* **80**, 181 (1998).
- <sup>26</sup>S. Dhar, O. Brandt, A. Trampert, K. J. Friedland, Y. J. Sun, and K. H. Ploog, *Phys. Rev. B* **67**, 165205 (2003).
- <sup>27</sup>W. Luo, S. R. Nagel, T. F. Rosenbaum, and R. E. Rosensweig, *Phys. Rev. Lett.* **67**, 2721 (1991).
- <sup>28</sup>W. S. Seo, H. H. Jo, K. Lee, B. Kim, S. J. Oh, and J. T. Park, *Angew. Chem., Int. Ed.* **43**, 1115 (2004).
- <sup>29</sup>R. Hoogerbeets, W. L. Luo, and R. Orbach, *Phys. Rev. Lett.* **55**, 111 (1985).
- <sup>30</sup>R. V. Chamberlin, G. Mozurkewich, and R. Orbach, *Phys. Rev. Lett.* **52**, 867 (1984).
- <sup>31</sup>C. N. Guy, *J. Phys. F: Met. Phys.* **8**, 1309 (1978).
- <sup>32</sup>G. Sinha, R. Chatterjee, M. Uehara, and A. K. Majumdar, *J. Magn. Magn. Mater.* **164**, 345 (1996).
- <sup>33</sup>R. S. Patel, D. Kumar, and A. K. Majumdar, *Phys. Rev. B* **66**, 54408 (2002).
- <sup>34</sup>W. H. Press *et al.*, *Numerical Recipes in C* (Cambridge University Press, Cambridge, 1992), p. 659.
- <sup>35</sup>S. H. Chun, Y. Lyanda-Geller, M. B. Salamon, R. Suryanarayanan, G. Dhalenne, and A. Revcolevschi, *J. Appl. Phys.* **90**, 6307 (2001).
- <sup>36</sup>P. Nordblad, P. Svedlindh, L. Lundgren, and L. Sandlund, *Phys. Rev. B* **33**, 645 (1986).
- <sup>37</sup>R. V. Chamberlin, *Phys. Rev. B* **30**, R5393 (1984).
- <sup>38</sup>L. Lundgren, P. Svedlindh, P. Nordblad, and O. Beckman, *Phys. Rev. Lett.* **51**, 911 (1983).
- <sup>39</sup>J. A. Mydosh, *Spin Glass* (Taylor and Francis, New York, 1993), pp. 75–76.
- <sup>40</sup>M. Suzuki, *Prog. Theor. Phys.* **58**, 1151 (1977).
- <sup>41</sup>S. Geschwind, D. A. Huse, and G. E. Devlin, *Phys. Rev. B* **41**, R2650 (1990).
- <sup>42</sup>K. H. Fischer and J. A. Hertz, *Spin Glasses* (Cambridge University Press, Cambridge, 1991), p. 260.
- <sup>43</sup>S. Mørup, M. B. Madsen, J. Franck, J. Villadsen, and C. J. W. Koch, *J. Magn. Magn. Mater.* **40**, 163 (1983); I. Tamura and M. Hayashi, *ibid.* **72**, 285 (1988); D. H. Reich, B. Ellman, J. Yang, T. F. Rosenbaum, G. Aeppli, and D. P. Belanger, *Phys. Rev. B* **42**, 4631 (1990).
- <sup>44</sup>It has been reported that 15 nm particles of NiO prepared by the same method as ours has a magnetic moment of  $700\mu_B$  [see R. H. Kodama, S. A. Makhlof, and A. E. Berkowitz, *Phys. Rev. Lett.* **79**, 1393 (1997)]. In the case of antiferromagnetic particles the moment  $\propto (\text{particle size})^n$  where  $n$  should be a number between 1 and 2 [see Néel (Ref. 5) or Richardson *et al.* (Ref. 13)]. Taking a value of  $n \sim 1.5$ , for the 5.1 nm sized particles, we estimate that the moment should be  $\sim 100\mu_B$ .
- <sup>45</sup>R. H. Kodama, A. E. Berkowitz, E. J. McNiff, Jr., and S. Foner, *Phys. Rev. Lett.* **77**, 394 (1996).
- <sup>46</sup>M. S. Seehra, V. S. Babu, A. Manivannan, and J. W. Lynn, *Phys. Rev. B* **61**, 3513 (2000).
- <sup>47</sup>P. Borrmann, O. Mülken, and J. Harting, *Phys. Rev. Lett.* **84**, 3511 (2000).